Dynamic Broadening of the Crystal-Fluid Interface of Colloidal Hard Spheres

Roel P. A. Dullens,* Dirk G. A. L. Aarts, and Willem K. Kegel
Van 't Hoff Laboratory for Physical and Colloid Chemistry, Debye Institute, Utrecht University, Padualaan 8, 3584 CH Utrecht, The Netherlands
(Received 20 June 2006; published 29 November 2006)

We investigate the structure and dynamics of the crystal-fluid interface of colloidal hard spheres in real space by confocal microscopy. Tuning the buoyancy of the particles allows us to study the interface close to and away from equilibrium. We find that the interface broadens from 8–9 particle diameters close to equilibrium to 15 particle diameters away from equilibrium. Furthermore, the interfacial velocity, i.e., the velocity by which the interface moves upwards, increases significantly. The increasing gravitational drive leads to supersaturation of the fluid above the crystal surface. This dramatically affects crystal nucleation and growth, resulting in the observed dynamic broadening of the crystal-fluid interface.

DOI: 10.1103/PhysRevLett.97.228301 PACS numbers: 82.70.Dd, 64.70.Dv, 68.08.−p

The long standing interest in the properties of crystal-fluid interfaces stems from their importance to many different fields ranging from physics to biology as well as metallurgy and surface science [1–6]. Interfacial properties direct processes such as crystal nucleation and growth [1–3,6–11], and many theoretical and computer simulation studies have demonstrated the particular importance of atomic-level structure on the thermodynamic properties of the crystal-melt interface [1,12–19]. In contrast to theory and simulations however, experimental studies are cumbersome as the crystal-fluid interface is embedded between two dense phases [1,6,14]. Despite this, investigations using high-resolution electron microscopy [20,21] and x-ray diffraction have provided significant insight [22,23]; however, these techniques cannot *directly* probe the structural dynamics at the single atom level. Because their relevant length and time scales are readily accessible in real space via confocal microscopy, colloidal systems provide an excellent model system for the study of interfaces [24]. In addition, colloids are widely accepted as a powerful model system for atomic and molecular systems [25] and statistical mechanics in general [26]. We take advantage of this here and investigate the structure of the hard-sphere crystal-fluid interface, comparing our results to the theoretical and computer simulation studies. This approach allows the exploration of both equilibrium and nonequilibrium structural and dynamical interfacial properties at the single particle, model atomic level.

We use monodisperse 1.45 μm diameter (d) polymethyl methacrylate spheres consisting of a fluorescent core and a nonfluorescent shell [27,28]. The particles are dispersed in an optically matching solvent mixture of *cis*-decalin, tetralin, and carbon tetrachloride, in which they behave as hard spheres [29]. By changing the composition of the solvent, the mass density difference $\Delta\rho_m$ with respect to the colloid's mass density (see Table I) is precisely controlled without changing the hard-sphere interaction. The initial volume fraction of colloids ϕ was 0.30 as defined relative to the volume fraction at random close packing [30]. Slow sedimentation induces particle accumulation and eventually crystallization at the bottom wall of the sample container. Subsequently, the crystal-fluid interface grows upwards due to the continuing sedimentation of particles [31]. Using a confocal microscope (Nikon Eclipse TE2000U with a Nikon C1 scanning head), we image a xyz-volume of typically $40 \times 40 \times 70$ μm^3 when the height (z) of the interface was approximately in the center of the imaged volume, i.e., ≈ 35 μm above the bottom wall of the sample container. We verified that the finite scanning speed of the microscope did not affect the measurements. Using particle tracking routines as described in [31,32], the three-dimensional centers of the particles were retrieved.

It is important to stress that we study crystal-fluid interfaces of systems that have not yet reached full sedimentation-diffusion equilibrium. Recall that the particles still sediment onto the interface, so the position of the interface changes in time. However, at the smallest mass density difference, the interface is almost stationary, and its local structure reflects the equilibrium interface. Hence, the mass density difference quantifies the proximity to the equilibrium situation: the system in solvent 1, smallest mass density difference, is closest to equilibrium, and in solvent 3, largest mass density difference, it is most out of equilibrium. The ratio between gravitational and thermal energy is given by the Peclet number: $\mathrm{Pe} = (4\pi\Delta\rho_m R^4 g)/(3k_B T)$, with $k_B T$ the thermal energy, g the acceleration due to gravity, and R the particle radius. Note

TABLE I. Characteristics of the solvents: the ratio tetralin/cis-decalin/carbon-tetrachloride ($v/v\%$), the mass density ρ_m, the mass density difference $\Delta\rho_m$, the viscosity η, and the Peclet number.

	composition	ρ_m (g/ml)	$\Delta\rho_m$ (g/ml)	η (mPa · s)	Pe
Solvent 1	36.0/31.5/32.5	1.146	0.024	2.04	0.066
Solvent 2	37.0/47.0/16.0	1.033	0.137	2.32	0.378
Solvent 3	31.0/69.0/−	0.914	0.256	2.78	0.707

that in all solvents $\mathrm{Pe} < 1$, which implies that thermal energy dominates gravity and hence, also hydrodynamic effects due to sedimentation.

In Fig. 1(a)–1(c), typical confocal microscopy images showing 2D xy-cross sections at different heights z are presented, where z' is rescaled such that the mean position of the interface is at $z' = 0$. A 2D xz-cross-section through the interface is presented in Fig. 1(d). At $z'/d \ll 0$ the crystalline region is encountered, Fig. 1(a). The in-plane hexagonal order is clearly recognized and corresponds to the close packed (111) crystal plane which is aligned parallel to the container bottom wall. Also, some vacancies are observed. In addition, the xz-slice [Fig. 1(d)] shows both fcc and hcp particle stackings in the crystalline region, indicating considerable randomness in the stacking of the hexagonal layers. Higher up in the sample, the hexagonal order is gradually lost and more disorder comes in; the interfacial region is entered [Fig. 1(b)]. Within one 2D cross section, ordered and disordered regions are observed, which implies that the crystal-fluid interface extends over more than one crystal plane and points towards a rough inhomogeneous interface. This is corroborated by the xz-slice, which shows that the crystalline stacking extents over different heights at various lateral positions. At $z'/d \gg 0$, a disordered structure is observed characteristic of the fluid region [Fig. 1(c)].

The reduced number density profiles along the z-direction $d^3\rho(z)$ for the three different solvents are shown in Fig. 2(a)–2(c). In all solvents, large periodic number density oscillations, reminiscent of the crystal, are observed at small heights. The oscillations gradually decrease when traveling from the crystalline region, through the interfacial region, to the fluid region. Finally, the structure in the number density profiles disappears in the fluid region. It is obvious from these profiles that the crystal-fluid interface extents over multiple particle diameters, consistent with the microscopy cross sections in Fig. 1. The number density profiles in the three solvents reveal a significant interfacial broadening upon increasing mass density difference. The interfaces are quantitatively described by fitting a tangent hyperbolic function to the envelope of the number density profiles [Fig. 2(a)–2(c)] (due to experimental uncertainties coarse-graining failed). The interfacial width is subsequently expressed in terms of the so-called 10–90 width $W_{10\text{–}90}$ [19], which is defined as the distance over which a parameter changes from 10% to 90% of its value in the crystal relative to its value in the fluid, as one traverses through the interface. Note that the vacancies in the crystalline region lower the interfacial width by about 4%. The averaged widths as a function of the mass density difference for the three solvents are presented in Fig. 2(d). The interfacial broadening is obvious, as the width increases from 8–9 particle diameters in solvent 1 to roughly 15 diameters in solvent 3. Figure 2(d) also shows the widths as determined from the in-plane hexagonal bond-order profiles, which exhibit the same broadening as the number density profiles. We note that the width obtained from the number density profiles is generally larger than the width determined from the bond-order profiles [19].

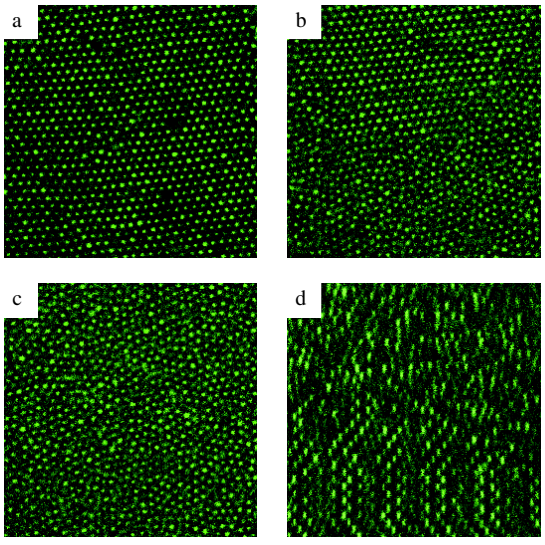

FIG. 1 (color online). Typical confocal microscopy images at different heights in the sample: (a) the crystalline ($z'/d = -18$), (b) the interfacial ($z'/d = 0$), and (c) the fluid region ($z'/d = 15$). (d) 2D xz-cross section through the interfacial plane. The size of the images is $40 \times 40\ \mu\mathrm{m}^2$.

As the position of the interface is almost stationary in solvent 1, the structure of the crystal-fluid interface closely resembles the structure of the equilibrium interface, which allows a direct comparison to theoretical and simulation studies. The interfacial width, being 8–9 particle diameters in solvent 1, may be extrapolated to the "equilibrium situation" at $\Delta\rho_m = 0$ g/ml. This yields an interfacial width of 7–8 particle diameters for the (111) hard-sphere crystal-fluid interface, which is in excellent agreement with simulations results [17–19]. Density functional theory generally predicts a smaller interfacial width for reasons not yet clear [16,17,19]. Furthermore, our data also reveal the coexistence of ordered and disordered regions within one 2D cross section in the interfacial region as observed in computer simulations of hard spheres and other simple liquids [12,13,19].

How the microscopic interfacial structure changes as the system is driven away from equilibrium—realized by increasing the mass density mismatch—is a rather unstudied issue. We anticipate that our observations may also be found in systems that are driven away from equilibrium by, e.g., electric or magnetic fields. The interfacial broadening inferred from Fig. 2(d) suggests that the roughness of the interface increases upon increasing mass density difference. At first sight, this is rather counterintuitive as one might expect the interface to be compressed if gravity is turned on. To elucidate the microscopic origin of the interfacial broadening, we identify the particles belonging to crystalline clusters using a local bond-order algorithm [33,34]. In Fig. 3(a)–3(c), computer reconstructions of the

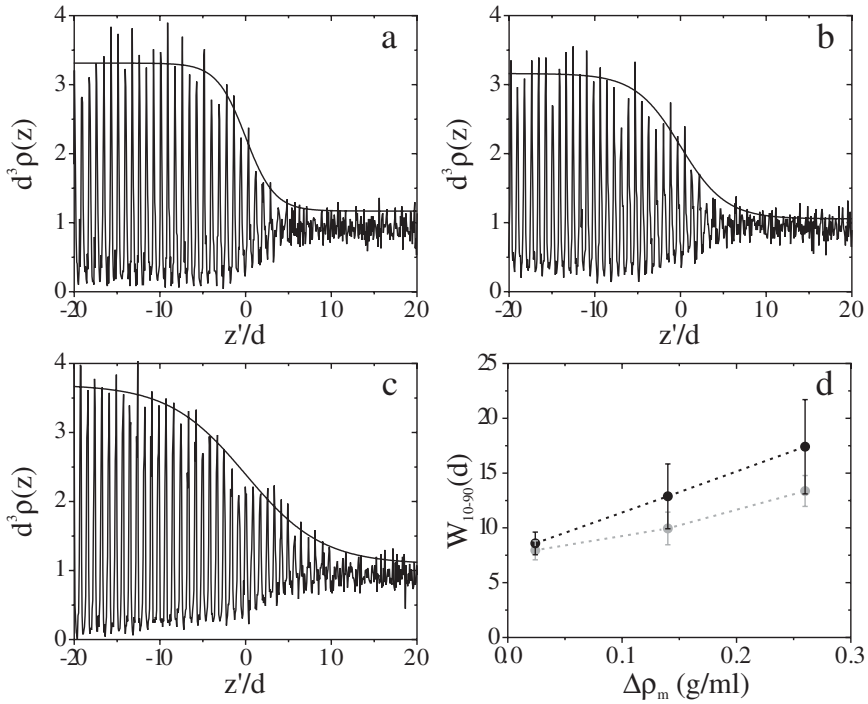

FIG. 2. Interfacial profiles and widths for the three different solvents. The reduced number density profiles $d^3\rho(z)$ for: (a) solvent 1, (b) solvent 2, and (c) solvent 3. The bin size for the number density profiles is 0.1 μm. The solid lines are hyperbolic tangent fits to the envelope of the number density profiles. (d) The averaged 10–90 widths W_{10-90} as a function of the mass density difference $\Delta\rho_m$ as obtained from the number density profiles (black) and the bond-order profiles (gray).

system in the three solvents are presented showing only the particles that are part of a crystalline cluster. Hence, these reconstructions directly visualize the structure of the crystal surface, i.e., the crystal-fluid interface. The change in the interfacial structure upon increasing mass density difference is obvious. The interface in solvent 1 [Fig. 3(a)] appears to be quite flat. The absence of crystallites above the crystal surface once more illustrates the equilibrium character of the interface at this smallest mass density difference. While already a few crystalline clusters in the fluid are observed in solvent 2 [Fig. 3(b)], a strong increase in the number of crystallites in the fluid region appears in solvent 3 [Fig. 3(c)]. Moreover, even if we discard the crystallites above the crystal surface, the increasing roughness of the interface itself is also evident from Fig. 3. Hence, the increasing number of crystallites that has already nucleated before they even reach the crystal surface suggests an increasing supersaturation of the fluid above the crystal surface. Indeed, measuring these volume fractions confirms the equilibrium number density of the fluid in solvent 1 ($\phi = 0.49$) and an increasing supersaturated nature of the fluid in solvents 2 ($\phi = 0.51$) and 3 ($\phi = 0.54$).

The dynamic properties of the crystal-fluid interface also change dramatically away from equilibrium. It is observed that the interfacial velocity, i.e., the velocity by which the interface moves upwards, clearly increases with increasing mass density difference (Fig. 4). The interfacial velocities in the three different solvents were determined by monitoring the evolution of the crystal-front in the xz-plane [24]. Naively, one may expect that the interfacial velocity is simply given by the sedimentation velocity of the particles at the initial volume fraction $u_s(\phi = 0.30)$ [25]. However, as observed in Fig. 4, only in solvent 1, the equilibrium situation, the interfacial velocity roughly equals the sedimentation velocity. Away from equilibrium, the sedimentation velocity exceeds the interfacial velocity. To

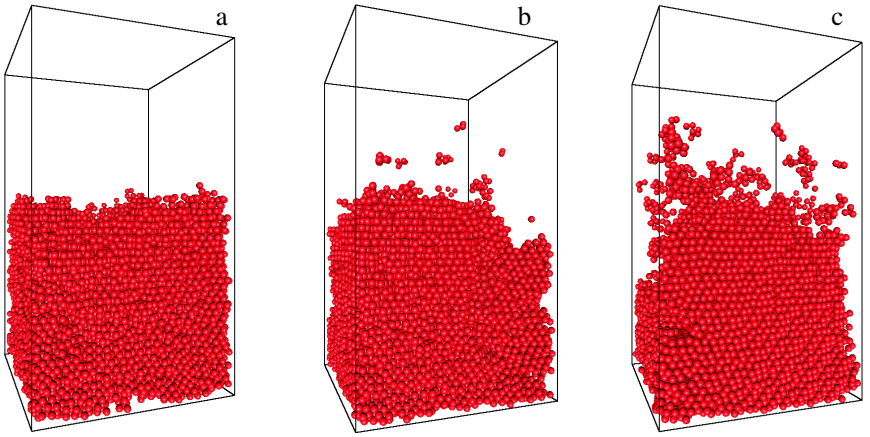

FIG. 3 (color online). Computer reconstructions of the crystal-fluid interfaces showing the particles that are part of a crystalline cluster: (a) solvent 1, (b) solvent 2, and (c) solvent 3. The xyz-dimensions of the boxes are $40 \times 40 \times 70$ μm^3.

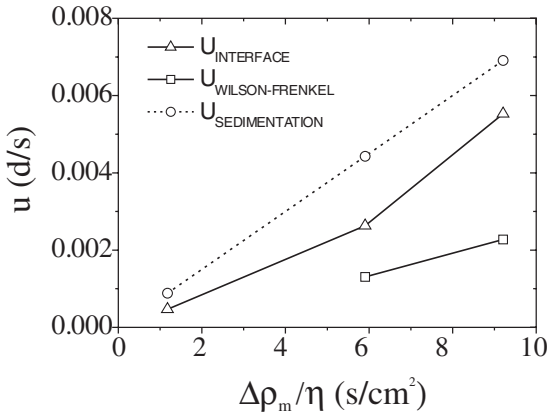

FIG. 4. The interfacial velocity (△), the crystal-growth velocity (□) as given by the Wilson-Frenkel law, and the sedimentation velocity (○) as a function of $\Delta\rho_m/\eta$, where η is the viscosity of the solvent (see Table I).

estimate the contribution of crystal growth to the interfacial velocity, we determine the crystal-growth velocity using the well-known Wilson-Frenkel law (see Fig. 4): $dz/dt = \alpha(D(\phi)/d)(1 - \exp[\Delta\mu/k_BT])$, with $D(\phi)$ the diffusion coefficient at the fluid volume fraction ϕ and $\Delta\mu$ the chemical potential difference between fluid and solid [7]. The diffusion coefficient is given by $D(\phi) \cong D_0(1 - \phi/0.64)^{1.17}$ and the parameter α is dimensionless and of order unity [7]. The crystal-growth velocity increases away from equilibrium, i.e., with increasing supersaturation. Note that crystal growth is absent in solvent 1 since $\Delta\mu \approx 0$ (no supersaturation). Furthermore, the crystal-growth speed is smaller than the interface velocity, and this difference significantly increases from solvent 2 to 3. As a result, the supersaturation of the fluid increases, resulting in many more crystal nucleii as observed in Fig. 3. Indeed, crystal nucleation is very sensitive to supersaturation: the crystal nucleation rate increases orders of magnitude if the fluid number density is increased only by a few percent [10,35]. Interestingly, the observed crystal nucleii are typically smaller than the critical nucleus size as reported in [7,10,35]. Therefore, these nucleii are expected to dissolve in time. However, they still contribute to the increasing roughness as they arrive at the crystal surface as ''ready-to-insert'' crystal packages. Whether the increase in roughness is related to a growth instability observed in [8,9] remains an open question. The absence of dendritic crystal growth in solvent 1 and the nucleation of crystallites in solvents 2 and 3 suggest at least a different mechanism.

We thank Jan van der Eerden, Daan Frenkel, and David Marr for helpful discussions and Urs Gasser for the bond-order parameter programs. This work is part of the research program of the Stichting voor Fundamenteel Onderzoek der Materie (FOM), financially supported by the Nederlandse Organisatie voor Wetenschappelijk Onderzoek (NWO).

*Electronic address: r.dullens@physik.uni-stuttgart.de.

[1] D. P. Woodruff, *The Solid-Liquid Interface* (Cambridge University Press, London, 1973).
[2] T. R. Thomas, *Rough Surfaces* (Longmans, London, 1982).
[3] J. M. Howe, *Interfaces in Materials* (Wiley, New York, 1997).
[4] A. W. Adamson and A. P. Gast, *Physical Chemistry of Surfaces* (Wiley, New York, 1997).
[5] W. J. Boettinger *et al.*, Acta Mater. **48**, 43 (2000).
[6] M. Asta, F. Spaepen, and J. F. van der Veen, MRS Bull. **29**, 920 (2004).
[7] B. J. Ackerson and K. Schätzel, Phys. Rev. E **52**, 6448 (1995).
[8] J. Zhu *et al.*, Nature (London) **387**, 883 (1997).
[9] W. B. Russel, P. M. Chaikin, W. V. Meyer, and R. Rogers, Langmuir **13**, 3871 (1997).
[10] S. Auer and D. Frenkel, Nature (London) **409**, 1020 (2001).
[11] U. Gasser *et al.*, Science **292**, 258 (2001).
[12] J. Tallon, Phys. Rev. Lett. **57**, 1328 (1986).
[13] J. Q. Broughton and G. H. Gilmer, J. Chem. Phys. **84**, 5749 (1986).
[14] B. B. Laird and A. D. J. Haymet, Chem. Rev. **92**, 1819 (1992).
[15] D. W. Marr and A. P. Gast, Phys. Rev. E **47**, 1212 (1993).
[16] R. Ohnesorge, H. Löwen, and H. Wagner, Phys. Rev. E **50**, 4801 (1994).
[17] A. Kyrlidis and R. A. Brown, Phys. Rev. E **51**, 5832 (1995).
[18] A. Mori, R. Manabe, and K. Nishioka, Phys. Rev. E **51**, R3831 (1995).
[19] R. L. Davidchack and B. B. Laird, J. Chem. Phys. **108**, 9452 (1998).
[20] S. E. Donnely *et al.*, Science **296**, 507 (2002).
[21] S. H. Oh *et al.*, Science **310**, 661 (2005).
[22] I. K. Robinson, Acta Crystallogr. Sect. A **54**, 772 (1998).
[23] E. Vlieg, Surf. Sci. **500**, 458 (2002).
[24] D. G. A. L. Aarts, M. Schmidt, and H. N. W. Lekkerkerker, Science **304**, 847 (2004).
[25] W. B. Russel and D. A. Saville, *Colloidal Dispersions* (Cambridge University Press, Cambridge, 1989).
[26] J. Perrin, *Les Atomes* (Libr. Felix Alcan, Paris, 1920).
[27] R. P. A. Dullens *et al.*, Langmuir **19**, 5963 (2003).
[28] R. P. A. Dullens, E. M. Claesson, and W. K. Kegel, Langmuir **20**, 658 (2004).
[29] R. P. A. Dullens, D. G. A. L. Aarts, and W. K. Kegel, Proc. Natl. Acad. Sci. U.S.A. **103**, 529 (2006).
[30] W. Schaertl and H. Sillescu, J. Stat. Phys. **77**, 1007 (1994).
[31] J. P. Hoogenboom, P. Vergeer, and A. van Blaaderen, J. Chem. Phys. **119**, 3371 (2003).
[32] J. C. Crocker and D. G. Grier, J. Colloid Interface Sci. **179**, 298 (1996).
[33] P. J. Steinhardt, D. R. Nelson, and M. Ronchetti, Phys. Rev. B **28**, 784 (1983).
[34] P. N. ten Wolde, M. J. Ruiz-Montero, and D. Frenkel, J. Chem. Phys. **104**, 9932 (1996).
[35] J. L. Harland and W. van Megen, Phys. Rev. E **55**, 3054 (1997).